Journal of Applied Electrochemistry **32**: 679–685, 2002.

Nano-scale copper-coated graphite as anode material for lithium-ion batteries

K. GUO, Q. PAN, L. WANG and S. FANG*
Institute of Chemistry, Chinese Academy of Sciences, Beijing, 100080, P.R. China
*(*author for correspondence, tel: +86 10 62562419, e-mail: fangsb@infoc3.icas.ac.cn)*

Received 23 October 2001; accepted in revised form 15 April 2002

Key words: electroless plating, graphite anode, nano-scale copper

Abstract

Nano-scale copper particles were homogeneously deposited on the surface of natural graphite through electroless plating. The co-intercalation of solvated lithium ion and reduction of the electrolyte were effectively depressed after coating of copper particles. Consequently, the graphite showed a significant improvement in charge–discharge properties such as coulombic efficiency, cycle characteristics, and high rate performance as an anode material for lithium ion batteries.

1. Introduction

Much attention has been focused on the anode material of lithium-ion batteries with the aim of obtaining high capacity, long cycling life and excellent high rate performance. Among various carbonaceous materials, natural graphite is the most attractive candidate because of its desirable charge–discharge curves and very low cost [1, 2]. However, large initial irreversible capacity and poor high rate performance have been problems associated with the application of natural graphite.

Generally, the initial irreversible capacity may arise from electrolyte reduction and subsequent formation of a solid electrolyte interface (SEI) film on the external surface of the graphite particles, and may also originate from cointercalation of solvated lithium ion between the graphite layers [3–8]. Poor high rate performance is due to the limited electrochemical reaction at the interface between graphite and electrolyte because migration of Li^+ took place only at the edge plane of graphite [9–11]. Therefore, much attention has been paid to the surface and interface condition of the graphite with respect to improvement of its electrochemical reaction rate [5, 12–15]. Recently, Takamura reported that an evaporated metal film had been deposited on the carbon surface and a different type of SEI film was formed, which evidently enhanced the electrochemical reaction rate at the interface between electrode and electrolyte [16].

In this paper, we report the electrochemical properties of a new type of natural graphite composite whose surface is homogenously covered by nano-scale copper particles by means of electroless plating.

2. Experimental details

The electroless deposition of copper particles on natural graphite was carried out by the following procedure at room temperature. Prior to copper deposition, graphite powder was initially sensitized by immersing in an aqueous solution of 0.1 M $SnCl_2$/0.1 M HCl, and then activated in an aqueous solution of 0.014 M $PdCl_2$/0.25 M HCl. Then, the graphite powder was dispersed and stirred in the plating solution containing 0.04 M $CuSO_4$, 0.12 M Ethylendiaminetetraacetic acid tetrasodium salt (EDTA), 0.08 M HCHO, 0.07 M Na_2SO_4 and 0.05 M HCOONa for 10 min. LiOH solution was used to adjust the pH to 12. After deposition, the graphite powder was rinsed with dionized water three times and dried at 100 °C under vacuum.

Preparation of graphite electrodes was carried out as described elsewhere [11]. The assembly of cells was carried out in a glove box filled with argon. The electrolyte used was 1 M solution of $LiPF_6$ dissolved in a mixture of ethylene carbonate (EC), diethyl carbonate (DEC) and propylene carbonate (PC) with different volume ratios. Charge–discharge cycling tests were conducted at different current densities in the potential range from 0.01 to 2.00 V vs Li/Li^+ using a computer-controlled battery tester. Cyclic voltammograms (CVs) were obtained using a three-electrode cell at a scan rate of 0.2 mV s^{-1}. Ac impedance measurements were carried out using IM6e impedance analyzer (Zahner Elektrik). Impedance spectra were measured by applying an ac voltage of 5 mV amplitude over the frequency range from 1 MHz to 10 mHz. Simulation of impedance

spectra with an equivalent circuit was performed using software 'SIM'. All the potentials indicated here were referred to Li/Li^+. The surface morphology of the graphite was investigated by scanning electron microscopy (SEM, S-530 Hitachi) and the amount of copper deposited was detected using an energy dispersive X-ray analytical system (EDAX).

3. Results and discussion

3.1. *Discharge–charge properties of copper coated graphite*

Figure 1 presents the scanning electron microscope images of the natural graphite (NG) and Cu-coated graphite. Clearly, copper particles with different sizes (300–50 nm) are deposited homogenously on the surface of the graphite particles, whereas the surface of the original natural graphite is smooth and bald.

Figure 2 shows the typical first discharge–charge (intercalation/deintercalation) profiles of the original natural graphite and Cu-coated graphite electrodes in 1 M $LiPF_6$ EC/DEC/PC (2:2:1 by volume). Compared with the natural graphite, the plateau at about 0.7 V in the discharge curve that is attributed to electrolyte reduction and the formation of SEI film [8] decreases for the Cu-coated graphite. Figure 3 illustrates the cyclic voltammograms for the natural graphite and Cu-coated graphite electrodes. The cathodic peaks corresponding to SEI film formation (0.9∼0.6 V) and cointercalation of solvated Li^+ (0.6∼0.3 V) [11] in the CVs of the copper-coated graphite are depressed compared to those of NG. These results indicate that the copper particles deposited can effectively suppress the electrochemical reaction caused by electrolyte reduction and cointercalation of solvated lithium ion.

3.2. *Cycling characteristic of copper coated graphite*

Typical cycle life (capacity vs cycle number) of the natural and Cu-coated graphite electrodes is shown in Figure 4. Evidently, the Cu-coated graphite electrode exhibits higher and more stable capacity than that of natural graphite electrode upon cycling. Difference in the cycling life between these two graphite electrodes can be explained by their impedance spectra, as shown in Figure 5. Figure 5 shows the electrochemical impedance spectra of the natural graphite and Cu-coated graphite electrodes at 0.2 V vs Li/Li^+ (lithium intercalation process) after different cycling numbers. It can be seen that there is a depressed semicircle in the high and middle frequency range in the impedance spectra. Upon cycling, the semicircle in the impedance spectra of the NG electrode increases distinctly (Figure 5(a)), whereas that of the Cu-coated graphite electrode almost remains unchanged (Figure 5(b)). As reported, the depressed semicircle in the middle frequency range is due to the charge transfer

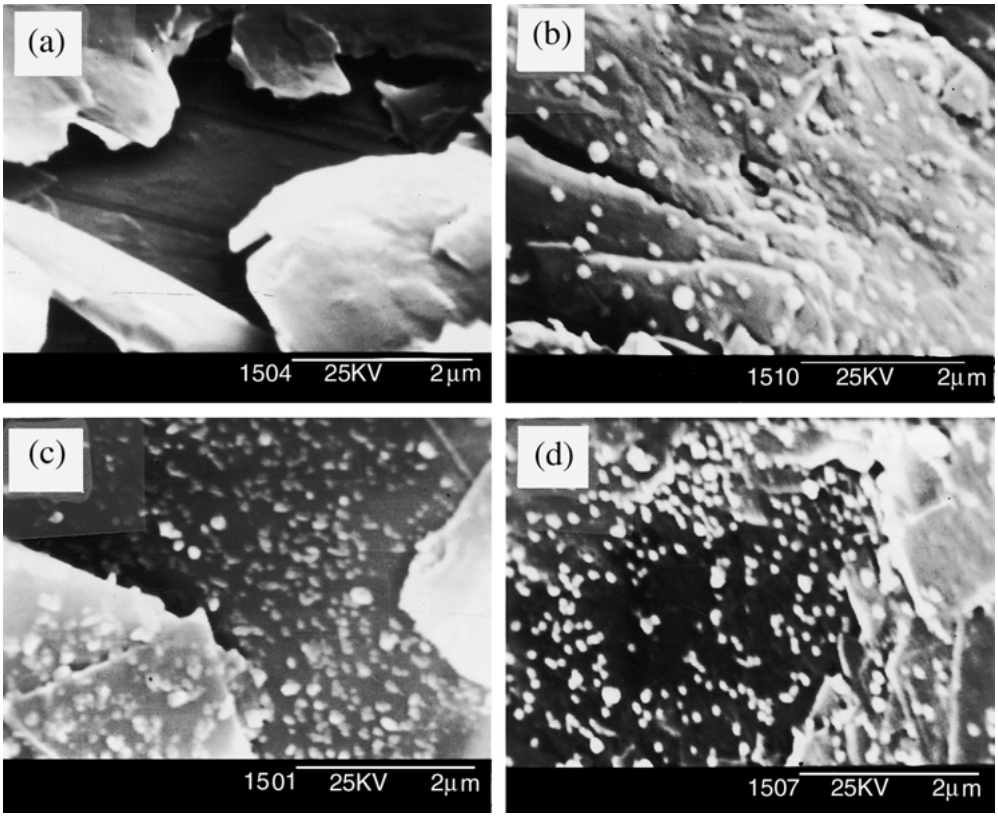

Fig. 1. Scanning electron microscope photographs of the graphite surface: (a) natural graphite; (b) 1.84 wt % Cu-coated graphite; (c) 3.09 wt % Cu-coated graphite; (d) 5.17 wt % Cu-coated graphite.

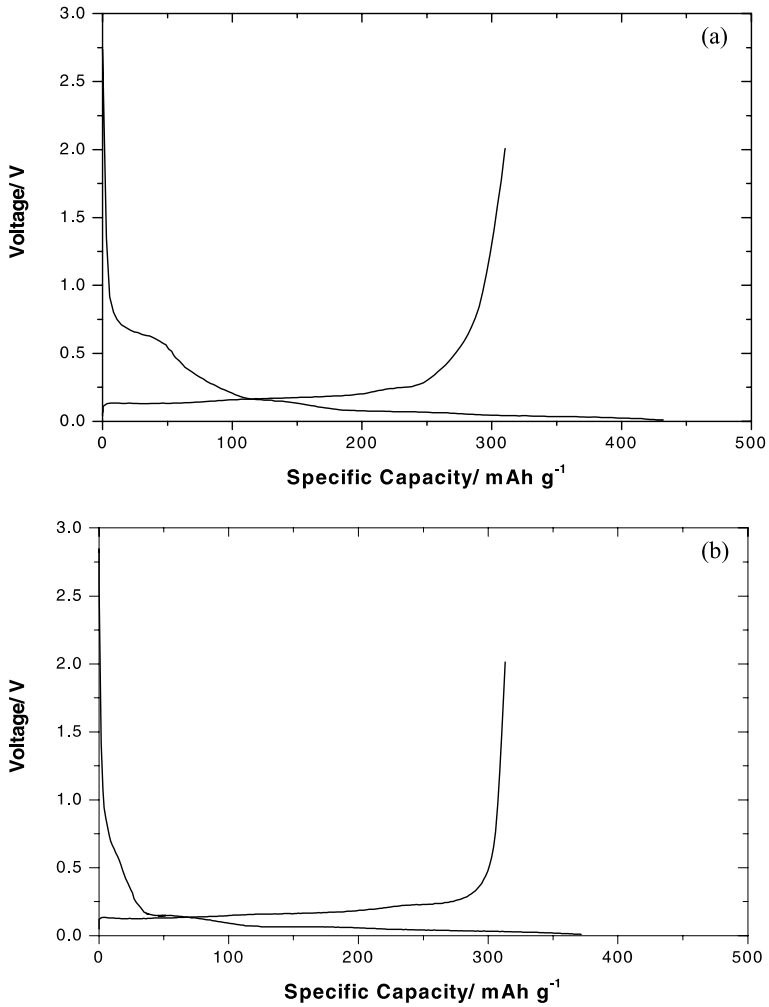

Fig. 2. Initial discharge–charge profiles of the graphite electrodes at a current density of 0.14 mA cm^{-2} in 1 M $LiPF_6$ EC/DEC/PC (2:2:1 by volume): (a) natural graphite; (b) 3.09 wt % Cu-coated graphite.

reaction at the interface between graphite and electrolyte. Maybe one capacity fading mechanism of the natural graphite electrode is a slowing of the electrode kinetics, as reflected by increasing charge transfer resistance upon prolonged cycling. This improved cycling behavior of the Cu-coated graphite electrode is due to the fact that its charge transfer resistance maintains constant (Figure 5(b)), thus maintaining stable electrochemical kinetics during repeated cycling.

3.3. *Effect of current densities on the discharge–charge properties of the Cu-coated graphite*

The charge (deintercalation) capacity of the natural and Cu-coated graphite electrodes at different current densities is presented in Figure 6. Overall, the charge capacity of the two electrodes decreases with increase in current density. However, the charge capacity of the Cu-coated graphite electrode fades more slowly than that of the natural graphite electrode as the current density increases. At a current density of 1.4 mA cm^{-2}, more than 100 mAh g^{-1} capacity difference is evident between two graphite electrodes, and the Cu-coated graphite still has a capacity of 208.4 mAh g^{-1}. These results show that high rate performance of the Cu-coated graphite electrode has been markedly improved. Improvement in the high rate performance of the Cu-coated graphite electrode can also be explained by its electrochemical impedance spectra, as shown in Figure 7. Two depressed semicircles in the high and middle frequency ranges are observed in the impedance spectra for both samples. As reported previously [17, 18], these two semicircles are ascribed to lithium ion migration through the SEI film (high frequency) and the charge-transfer reaction at the interface between graphite and electrolyte (middle frequency), respectively. Obviously, the semicircles of the Cu-coated graphite are smaller than those of the natural graphite. The smaller impedance in the high-frequency semicircle of the Cu-coated graphite indicates that the lithium ion conduction rate in the SEI film is enhanced. Meanwhile, lower charge-transfer resistance for the Cu-coated graphite implies that copper deposited is favorable for lithium ion charge-transfer at the graphite–electrolyte interface. These results clearly show that these copper particles deposited on the graphite surface have a

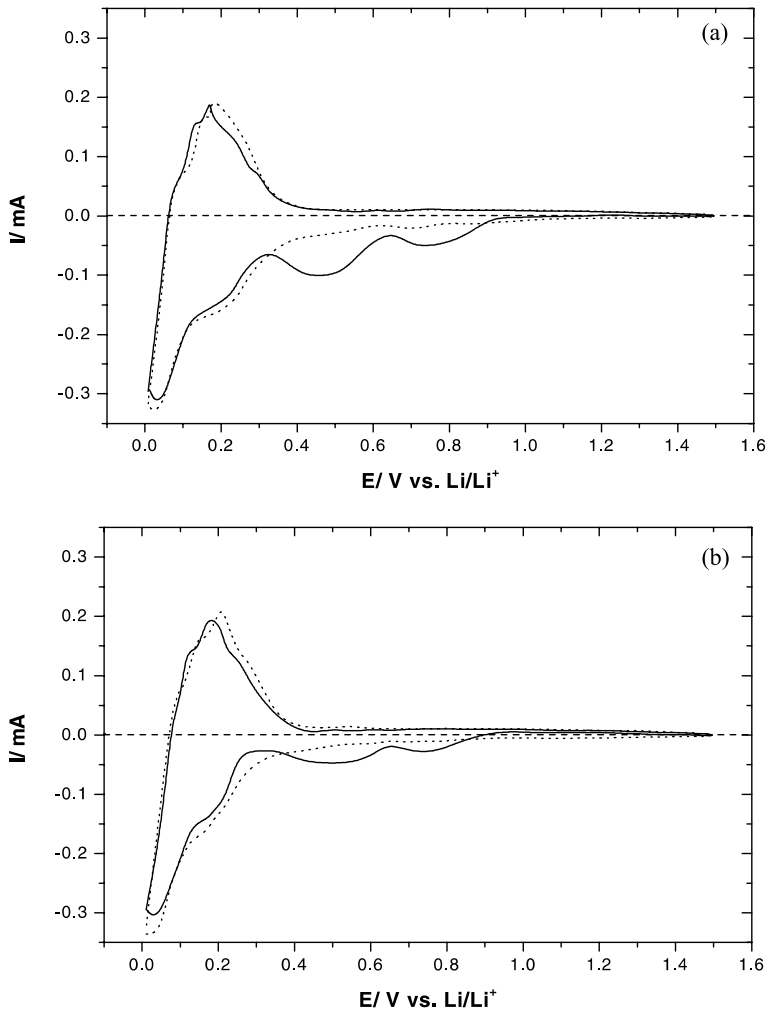

Fig. 3. Cyclic voltammograms of graphite electrodes in 1 M $LiPF_6$ EC/DEC/PC (2:2:1 by volume): (a) natural graphite; (b) 3.09 wt % Cu-coated graphite, scan rate 0.2 mV s^{-1}. Key: (—) 1st cycle; (···) 2nd cycle.

beneficial effect on the diffusion of lithium ion into the graphite structure. As a result, the electrochemical reaction rate of the Cu-coated graphite electrode is enhanced, thus improving its high rate performance.

3.4. *Effect of copper amount on the electrochemical properties of graphite*

Table 1 lists the initial coulombic efficiency and charge capacity of the graphite electrodes with different copper amounts. As the copper coating amount increases, the initial discharge capacity of the Cu-coated graphite electrodes decreases substantially and the initial coulombic efficiency increases. The decreasing intercalation capacity is due to the fact that cointercalation of the solvated lithium ion is depressed by the copper particles, as revealed by cyclic voltammograms. As the copper amount increases, it protects the graphite electrodes from the solvated lithium ion intercalation more effectively. As a result, the initial discharge capacity of the Cu-coated graphite decreases and the initial coulombic efficiency increases. However, after 8.20 wt % copper is deposited, both the deintercalation capacity and initial coulombic efficiency of the Cu-coated graphite drop. The levelling off of the deintercalation capacity and initial coulombic efficiency is due to a decrease in the amount of active material for reversible Li intercalation/deintercalation in the copper coated graphite. As seen from Table 1, the more copper particles were deposited on the graphite surface, the less was influence of the current density on the charge capacity of the Cu-coated graphite. This is because the greater the number of copper particles deposited, the higher the electrochemical reaction at the interface.

3.5. *Effect of PC concentration on the electrochemical properties of graphite*

To gain more insight into the electrochemical performance of the Cu-coated graphite, the discharge–charge properties of the Cu-coated graphite electrodes in electrolytes with different PC concentrations are presented in Table 2. The higher the PC content the larger the irreversible capacity and the lower the initial coulombic efficiency. In addition, it can be seen that as the coating amount increases, the irreversible capacity of

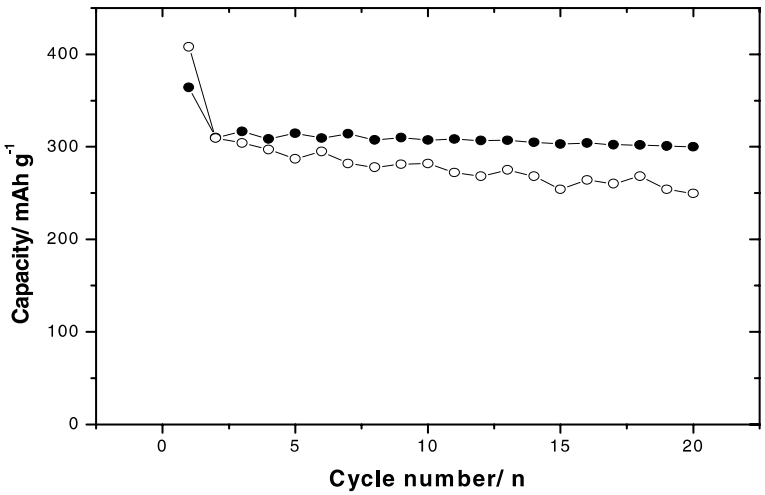

Fig. 4. Cycling characteristics of the natural and 3.09 wt % Cu-coated graphite at a current density of 0.14 mA cm^{-2} in 1 M $LiPF_6$ EC/DEC/PC (2:2:1 by volume). Key: (●) Cu-covered graphite; (○) natural graphite.

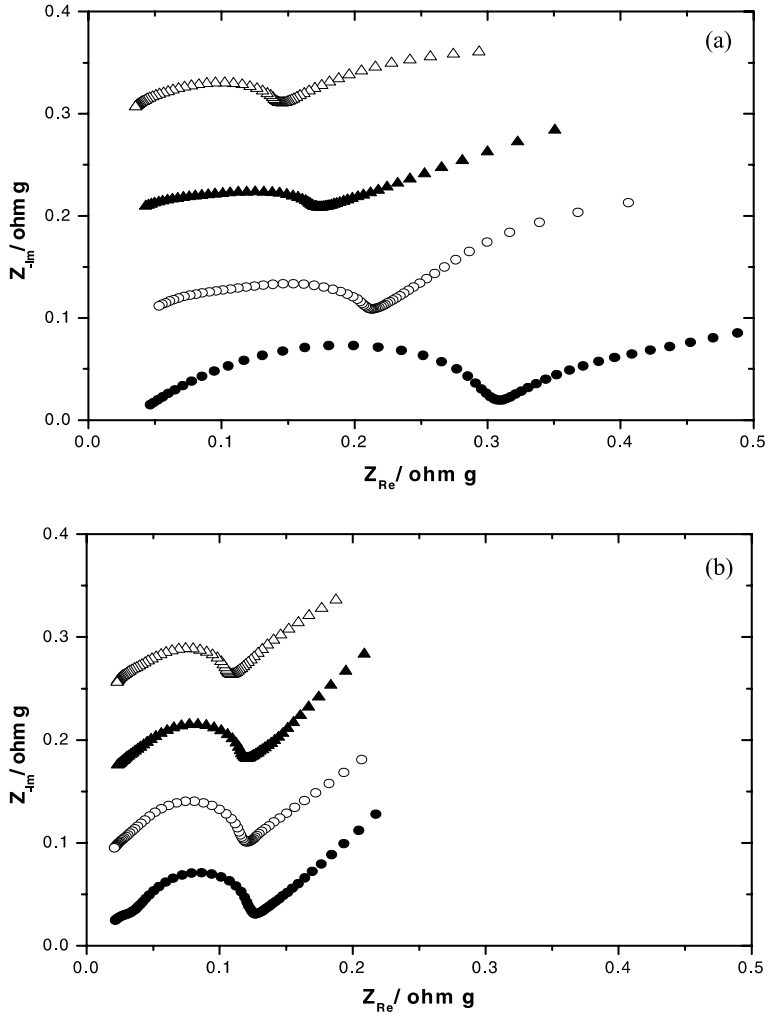

Fig. 5. Impedance spectra measured with natural and Cu-coated graphite electrodes after different cycles at 0.2 V (lithium intercalation process) in 1 M $LiPF_6$ EC/DEC/PC (2:2:1 by volume): (a) natural graphite; (b) Cu-coated graphite. Average particle size = 20 μm, 7% PVDF (by weight), electrode thickness = 50 μm (a copper grid was used as a current collector). Key: (●) 20 cycles; (○) 15 cycles; (▲) 10 cycles; (△) 2 cycles.

the Cu-coated graphite becomes smaller for each electrolyte. This shows that the copper particles depress the irreversible capacity of the natural graphite in PC-based electrolytes.

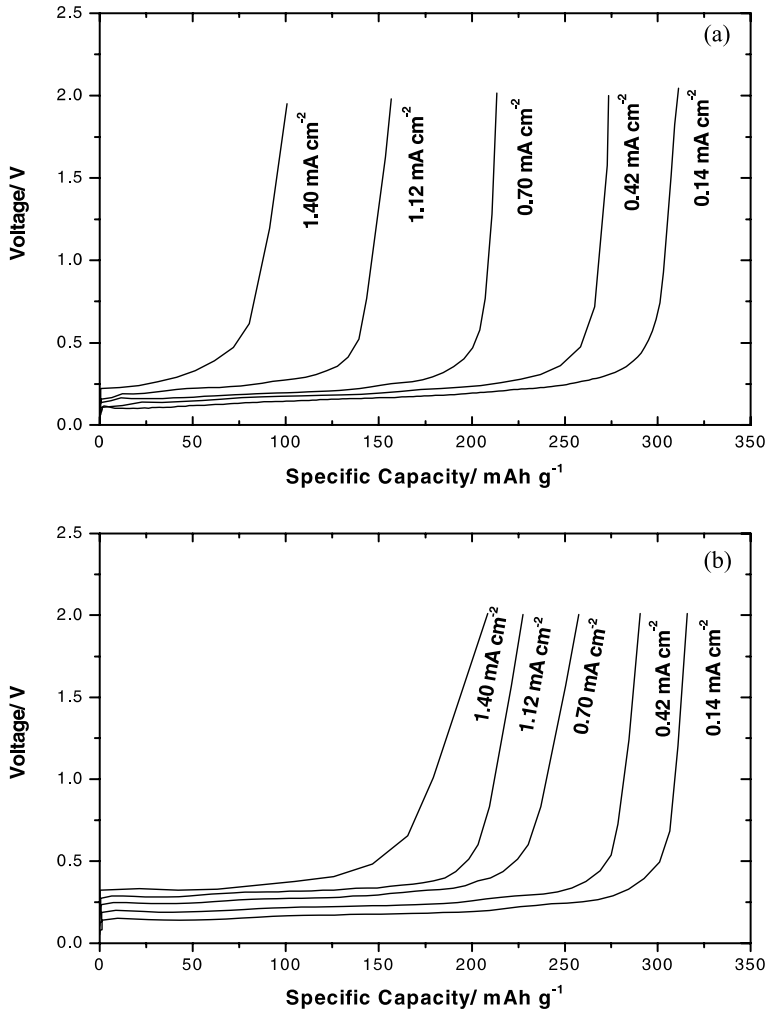

Fig. 6. Charge profiles of the natural and Cu-coated graphite at different current densities in 1 M $LiPF_6$ EC/DEC/PC (2:2:1 by volume): (a) natural graphite; (b) 3.09 wt % Cu-coated graphite.

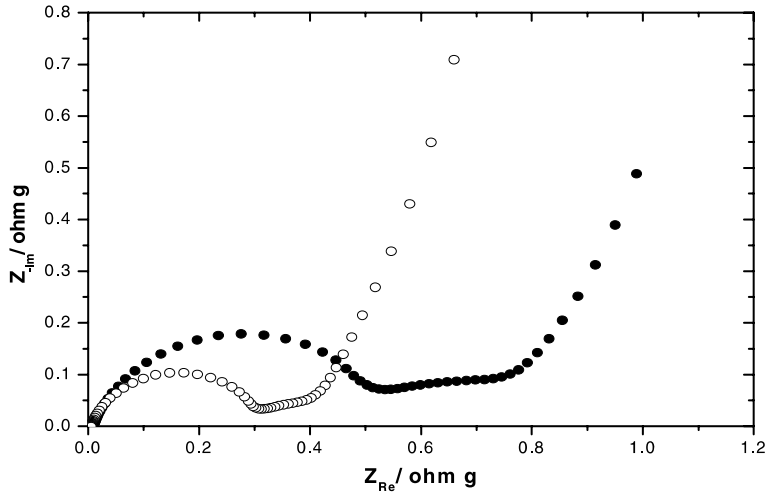

Fig. 7. Impedance spectra measured with natural and Cu-coated graphite electrodes at 0.2 V of the 1st intercalation in 1 M $LiPF_6$ EC/DEC/PC (2:2:1 by volume): (a) natural graphite; (b) 3.09 wt % Cu-coated graphite. Average particle size = 20 μm, 7% PVDF (by weight), electrode thickness = 50 μm (A copper grid was used as a current collector). Key: (●) natural graphite; (◯) Cu-coated graphite.

4. Conclusion

To improve the electrochemical performance of natural graphite, nano-scale copper particles were deposited on the surface of natural graphite via electroless plating. The graphite obtained showed great improvement in electrochemical performance, such as the initial coulombic efficiency and cycle characteristic. The high rate

Table 1. Electrochemical properties of graphite electrodes orderly at different current densities in 1 M $LiPF_6$ EC/DEC/PC (2:2:1 by volume)

Sample	NG	1.84 wt % Cu	3.09 wt % Cu	5.17 wt % Cu	8.20 wt % Cu
1st cycle efficiency/%	71.8	77.3	82.6	84.2	80.3
1st discharge capacity/ mAh g^{-1}, 0.14 mA cm^{-2}	431.0	394.7	380.7	367.8	326.5
1st charge capacity/mAh g^{-1}, 0.14 mA cm^{-2}	309.4	305.1	314.5	309.2	262.2
6th charge capacity/mAh g^{-1}, 0.42 mA cm^{-2}	273.2	288.8	290.6	281.5	247.3
11th charge capacity/mAh g^{-1}, 0.70 mA cm^{-2}	214.1	245.6	257.6	260.8	218.6
16th charge capacity/mAh g^{-1}, 1.12 mA cm^{-2}	156.7	215.8	227.4	226.1	185.2
21st charge capacity/mAh g^{-1}, 1.40 mA cm^{-2}	102.3	150.2	208.4	207.5	157.5

Table 2. Electrochemical properties of natural and Cu-coated graphite electrodes at a current density of 0.14 mA cm^{-2} in electrolytes with different concentrations of PC (by volume)

Electrolyte	*	Sample			
		NG	1.84 wt % Cu	3.09 wt % Cu	5.17 wt % Cu
1 M $LiPF_6$ + EC:DEC:PC (2:2:1)	Q_d/mAh g^{-1}	431.0	394.7	380.7	367.8
	Q_c/mAh g^{-1}	309.4	305.1	314.5	309.7
	Q_{irr}/mAh g^{-1}	121.6	89.6	66.2	58.1
	η/%	71.8	77.3	82.6	84.2
1 M $LiPF_6$ + EC:DEC:PC (1.5:1.5:1)	Q_d/mAh g^{-1}	459.4	429.9	404.3	387.8
	Q_c/mAh g^{-1}	306.9	308.7	312.9	312.5
	Q_{irr}/mAh g^{-1}	152.5	121.2	91.4	75.3
	η/%	66.8	71.8	77.4	80.6
1 M $LiPF_6$ + EC:DEC:PC (1:1:1)	Q_d/mAh g^{-1}	481.8	442.7	421.2	403.5
	Q_c/mAh g^{-1}	178.5	299.7	308.3	304.3
	Q_{irr}/mAh g^{-1}	203.3	143.0	112.9	99.2
	η/%	57.8	67.7	73.2	75.4
1 M $LiPF_6$ + EC:DEC:PC (1:1:2)	Q_d/mAh g^{-1}	502.6	471.0	428.3	414.3
	Q_c/mAh g^{-1}	250.3	289.1	295.1	298.7
	Q_{irr}/mAh g^{-1}	252.3	181.9	133.2	115.6
	η/%	49.8	61.4	68.9	72.1

*Q_d: the discharge capacity in the first cycle; Q_c: the charge capacity in the first cycle; Q_{irr}: the irreversible capacity in the first cycle; η: the initial coulombic efficiency.

performance of the Cu-coated graphite was also improved due to the acceleration of charge transfer reaction during Li^+ intercalation. The results of this study demonstrate that natural graphite coated by nanoscale copper particles is an excellent candidate anode material for lithium-ion batteries.

Acknowledgements

The authors would like to thank Dr Yongfang Li for discussion and support during the preparation of this work. The authors also acknowledge the Natural Sciences Fund of China (50 173 029), for financial support.

References

1. T. Nagaura, 4th International Rechargeable Battery Seminar, Deerifield Beach, FL (1990).
2. Y. Masaki, W. Hongyu and F. Kenji, *J. Electrochem. Soc.* **147** (2000) 1245.
3. R. Fong, U. von Sacken and J.R. Dahn, *J. Electrochem. Soc.* **137** (1990) 2009.
4. D. Aurbach, Y. Ein-Eli and Y. Carmeli, *J. Electrochem. Soc.* **141** (1994) 603.
5. E. Peled, G. Manchem and D. Bar-Tow, A. Melman, *J. Electrochem. Soc.* **143** (1996) L4.
6. M. Winter, P. Novak and A. Monnier, *J. Electrochem. Soc.* **145** (1998) 428.
7. G. Chung, S. Jun, K. Lee and M. Kim, *J. Electrochem. Soc.* **146** (1999) 1664.
8. D. Aurbach, *J. Power Sources* **89** (2000) 206.
9. J.O. Besenhard, M. Winter, J. Yang and W. Biberacher, *J. Power Sources* **54** (1995) 228.
10. T.D. Tran, J.H. Feikert, X. Song and K. Kinoshita, *J. Electrochem. Soc.* **142** (1995) 3297.
11. P. Yu, J.A. Ritter, R.E. White and B.N. Popov, *J. Electrochem. Soc.* **147** (2000) 1280.
12. Z.L. Liu, A. Yu and J.Y. Lee, *J. Power Sources* **81–82** (1999) 187.
13. C. Menachem, E. Peled, L. Burastein and Y. Rosenberg, *J. Power Sources* **68** (1997) 277.
14. S. Ahn, Y. Kim and K. Joon Kim, *J. Power Sources* **81–82** (1999) 896.
15. Q.M. Pan and S.B. Fang, '*Polymers for Advanced Technologies*,' (in press).
16. T. Takamura, K. Sumiya and K. Sekine, *J. Power Sources* **81–82** (1999) 368.
17. W.W. Huang and R. Frech, *J. Electrochem. Soc.* **145** (1998) 765.
18. E. Barsoukov, J.H. Kim and C.O. Yoon, *Solid State Ionics* **116** (1999) 249.